Single-Molecule Conductance of Pyridine-Terminated Dithienylethene Switch Molecules

Eugenia S. Tam,[†] Joshua J. Parks,[†,‡] William W. Shum,[‡] Yu-Wu Zhong,[§] Mitk'El B. Santiago-Berríos,[‡] Xiao Zheng,[⊥] Weitao Yang,[⊥] Garnet K.-L. Chan,[‡] Héctor D. Abruña,[‡] and Daniel C. Ralph[†,¶,*]

[†]Laboratory of Atomic and Solid State Physics, [‡]Department of Chemistry and Chemical Biology, and [¶]Kavli Institute at Cornell, Cornell University, Ithaca, New York 14853, United States, [§]Institute of Chemistry, Chinese Academy of Sciences, Beijing 100190, PRC, and [⊥]Department of Chemistry, Duke University, Durham, North Carolina 27708, United States.

ABSTRACT We have investigated the conductance of individual optically switchable dithienylethene molecules in both their conducting closed configuration and nonconducting open configuration, using the technique of repeatedly formed break-junctions. We employed pyridine groups to link the molecules to gold electrodes in order to achieve relatively well-defined molecular contacts and stable conductance. For the closed form of each molecule, we observed a peak in the conductance histogram constructed without any data selection, allowing us to determine the conductance of the fully stretched molecules. For two different dithienylethene derivatives, these closed-configuration conductances were $(3.3 \pm 0.5) \times 10^{-5}\ G_0$ and $(1.5 \pm 0.5) \times 10^{-6}\ G_0$, where G_0 is the conductance quantum. For the open configuration of the molecules, the existence of electrical conduction *via* the molecule was evident in traces of conductance *versus* junction displacement, but the conductance of the fully stretched molecules was less than the noise floor of our measurement. We can set a lower limit of 30 for the on/off ratio for the simplest dithienylethene derivative we have investigated. Density functional theory calculations predict an on/off ratio consistent with this result.

KEYWORDS: molecular electronics · single molecule conductance · photochromism · optoelectronics · electronic transport · molecular switch · dithienylethene

In the development of molecular and nanoscale electronics, there is an active search for molecules whose electrical conductance is optically switchable, which might open the possibility of integrated opto-electronic devices. Especially promising are diarylethenes, a class of photochromic molecules that can reversibly change configuration back and forth between two different conductance states by irradiation with specific wavelengths of light[1] as well as by electrochemical methods.[2] The high-conductance conjugated isomer (hereafter referred to as the "closed" or **c** form) can be switched by visible light to the low-conductance unconjugated isomer ("open" or **o** form). The reverse process occurs under ultraviolet (UV) irradiation. For applications in both thin-film solid-state devices and in single-molecule junctions, diarylethenes are particularly attractive because of their thermal stability, high fatigue resistance, and sub-angström difference in length between isomers.[3] This last characteristic is particularly important due to the strong dependence of conduction with molecular length.

Experimental approaches to investigate electronic transport through diarylethene derivatives have included mechanically controllable break-junctions,[4] self-assembled monolayers with macroscopic electrodes,[5] scanning tunneling microscopy (STM),[6,7] attachment to single-walled carbon nanotube electrodes,[8] and incorporation into metal nanoparticle networks.[9,10] Key findings include on/off conductance ratios ranging from 10 to 100 and the irreversibility of switching for certain derivatives when attached to Au electrodes. Ensuing theoretical analysis predicted the conduction to be HOMO-dominated with conductance on/off ratios ranging from 20 to several hundred, in reasonable agreement with experiment.[11−14] The calculated conductances varied, with some predictions for the closed forms of thiol-terminated derivatives as high as $0.6-0.7\ G_0$,[11,12] (where G_0 is the conductance quantum, $2e^2/h \approx (12.9\ \mathrm{k}\Omega^{-1})$) much higher than the experimentally measured values which are on the order of $10^{-3}\ G_0$.[4,6] However, conductance overestimation is common in density functional theory (DFT) calculations.[15] The irreversibility of open-to-closed switching of some derivatives when attached to Au electrodes was attributed to the much lower energy of the HOMO for the open form, so excited states are quenched by the coupling to a metallic reservoir. For reviews of the synthesis and properties of diarylethenes, see refs 1, 3, 16, and 17.

Previous studies of the conductance properties of diarylethenes have reported results from a limited number of devices

* Address correspondence to ralph@ccmr.cornell.edu.

Received for review March 30, 2011 and accepted May 16, 2011.

Published online May 16, 2011
10.1021/nn201199b

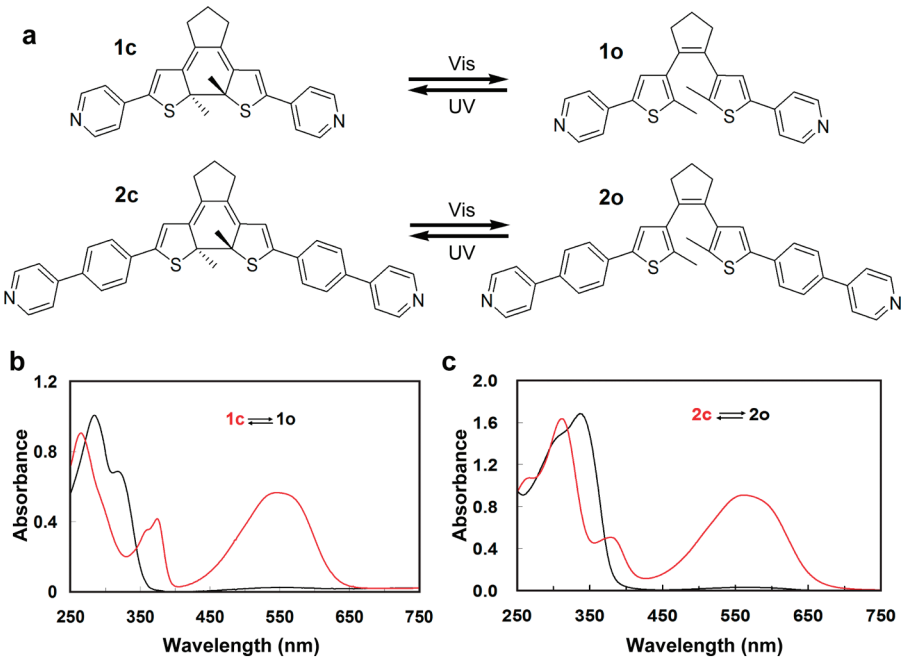

Figure 1. (a) Isomers of the pyridine-terminated dithienylethene derivatives investigated in this work. (b,c) UV−vis absorbance of molecule 1o/c (b) and molecule 2o/c (c).

incorporating either individual molecules[4,7] or an ensemble of molecules.[5,9,10] Because fluctuations in the junction geometry can lead to exponential variations in molecular conductance, meaningful information can best be obtained statistically, for example, by repeated formation of molecular junctions.[18,19] A statistical study of a thiol-terminated dithienylethene derivative reported conductance values obtained from histograms constructed from a selected subset of traces for which a low-conductance plateau was evident.[6] However, recent work by Venkataraman *et al.* has shown that consistent and reproducible results can, in fact, be obtained without any data selection for molecules terminated with certain linker groups (including amine, phosphine, and pyridine) which yield well-defined conductance values, in contrast to molecules terminated with thiol and isonitrile end-groups.[20] Here, we report on measurements of the conductance of pyridine-terminated dithienylethenes without any trace selection, thus capturing the full range of possible junction geometries. We find a conductance value for the closed isomer **1c** (Figure 1a) of $(3.3 \pm 0.5) \times 10^{-5}$ G_0 and a lower bound for the on/off conductance ratio of 30. In contrast to simpler pyridine-terminated molecules,[21,22] we observe that the closed dithienylethene isomer does not exhibit bistable conducting configurations due to two well-defined bonding motifs. We attribute this to the overlap of the conductance ranges for the two bonding motifs known for pyridine groups, as supported by DFT calculations.

RESULTS AND DISCUSSION

We prepared compounds **1o** and **2o** (Figure 1a) according to known procedures.[23−25] The synthesis details are described in the Methods section. These dithienylethene-based molecules are terminated with pyridine end-groups to facilitate binding to the Au metal leads and to promote well-defined conductance values in statistical measurements.[20] Compound **2o** is designed with an additional phenyl spacer between the switch unit and each pyridine group, compared to compound **1o**. We were motivated to study this molecule by the report of reversible switching of a similar molecule when bound to Au electrodes in ref 7.

Figures 1b and 1c show the UV−vis absorption spectrum of the open and closed forms of molecules **1** and **2**. As prepared, the solution contains mostly molecules in the open form, showing negligible absorbance at wavelengths above 350 nm (black curves in Figure 1b,c). After UV-irradiation (λ = 380 nm; power density approximately 1500 μW/cm^2) for 15 min, most of the molecules isomerize to the closed, conjugated form, and a prominent peak appears in the visible region of the spectrum (red curves). The reaction is reversible by irradiation at λ = 500−600 nm.

Our experimental procedures for measuring molecular conductances follow those described previously by the Venkataraman group at Columbia University[18,21] and are detailed in the Methods section. Briefly, a freshly cut Au tip is brought into and out of contact with a Au substrate (prepared by evaporation onto an oxidized Si wafer) by a piezoelectric-based actuator. A drop of a dilute solution (<1 mM) of the molecule in 1,2,4-trichlorobenzene (Sigma-Aldrich) is deposited at the junction. In a typical measurement, the tip is biased at 50 mV and retracted at 8−16 nm/s at room

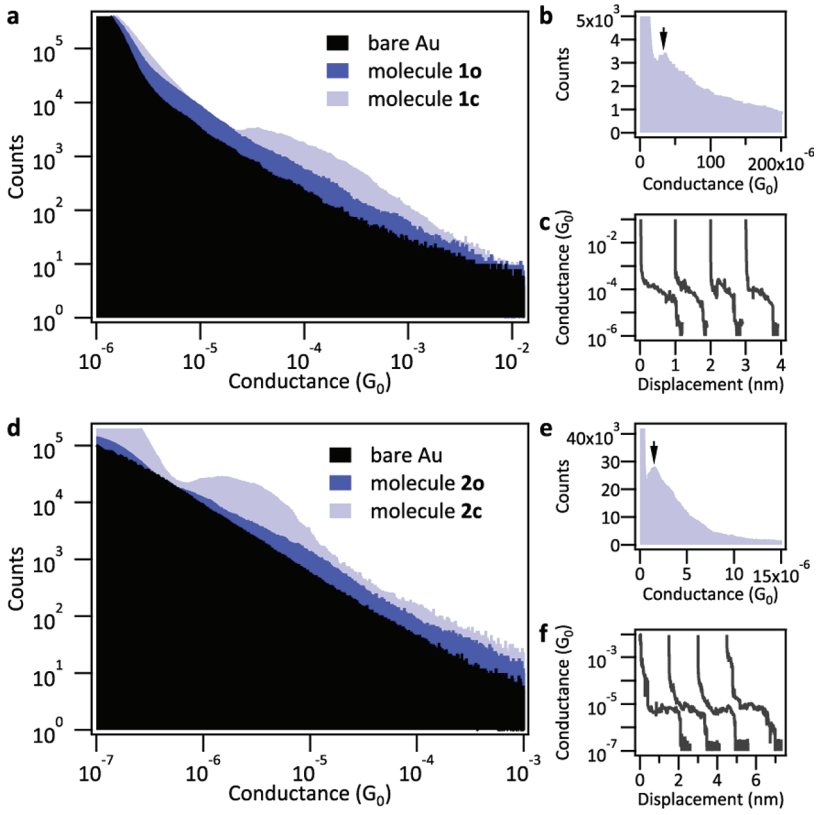

Figure 2. (a) Conductance histograms for bare Au electrodes in pure solvent (black), molecule 1o (dark blue), and molecule 1c (light blue) plotted on a log−log scale. (b) Isolated histogram for molecule 1c on a linear−linear scale. Arrow indicates approximate peak location. (c) Individual traces of conductance *versus* junction displacement for molecule 1c. Plateaus in the 10^{-5} G_0 range are clearly visible. (d−f): Same as panels a−c, respectively, for molecule 2o/c.

temperature. The current is recorded at 40 kHz. Histograms are constructed from thousands of traces without any data selection. As a test of the capabilities of our apparatus, we first performed measurements on several molecules for which detailed results have been published previously by the Venkataraman group, including several diaminoalkanes and 4,4′-bipyridine. Our results (provided in the Supporting Information) are in excellent quantitative agreement with the previously published data.[18,21,26,27] This confirms that consistent results for single molecule conductance can be obtained without trace selection.

Figure 2a shows overlaid conductance histograms in the range of 10^{-6} to 10^{-2} G_0 for bare Au electrodes in pure 1,2,4-trichlorobenzene solvent and for Au electrodes in contact with solutions of dithienylethene derivatives **1o** and **1c**. The histograms are constructed from 1000 traces each with uniform bins of width 1×10^{-7} G_0 but are plotted on a log−log scale, for clarity, in Figure 2a. The histogram for compound **1c** (closed isomer) shows a well-defined conductance peak not present in either the histogram for bare Au or compound **1o**. We fit the conductance peak for **1c** (Figure 2b) to a Lorentzian function and find a junction conductance of $(3.3 \pm 0.5) \times 10^{-5}$ G_0. The peak is relatively broad (2 orders of magnitude in conductance), suggesting contributions from a variety of different molecular geometries. This variability in geometry is also directly evident in the individual conductance *versus* displacement traces like those shown in Figure 2c. In most of the traces (over 70%), we see a clear sloping plateau with the conductance decreasing continuously as the junction is pulled apart, starting at values as high as 10^{-3} G_0 and breaking abruptly in the 10^{-5} G_0 range. We believe that this conductance plateau corresponds to the formation and elongation of a molecular junction. As will be discussed in more detail later in this paper, we interpret the histogram peak value to represent the most probable conductance of the fully stretched molecular junction. In contrast, for the open form of the molecule (**1o**) we were not able to measure a peak in the histogram within our conductance measurement limit of 10^{-6} G_0 (see Experimental Details in the Supporting Information). However, in the individual traces (Figure S5 in the Supporting Information) one can see that there is a measurable current in the **1o** junctions that decreases continuously to our noise level within a shorter displacement distance than the typical width of the conductance plateaus for **1c**, suggesting that the conductance of the fully stretched **1o** molecule is below our experimental noise floor. We will discuss these observations further in later sections of this paper.

Figure 2 panels d–f show the corresponding data for compounds **2o** and **2c**, which have an additional phenyl ring between the central switching unit and each of the pyridine anchor groups. A Lorentzian fit to the peak in the histogram for **2c** (Figure 2e) yields a conductance of $(1.5 \pm 0.5) \times 10^{-6}\ G_0$, which is 22 times smaller than that for **1c**. This decrease in conductance is in reasonable agreement with a naïve expectation based on previously reported results of conjugated molecules (specifically oligophenyldiamines) of a conductance decay constant of 1.7 per phenyl ring,[20] which predicts a 29-fold decrease for two rings. We synthesized and measured compound **2o** to demonstrate the possibility of further decoupling the switching unit from the electrodes. In the remainder of this paper, we focus on a more-detailed analysis of data for compounds **1o** and **1c**.

Although the dithienylethene derivatives that we employed are different from those in refs 4 and 6, it is worth noting that the conductance we measure for **1c** is 2 orders of magnitude less than the conductance values reported in those works (on the order of $10^{-3}\ G_0$ for the closed isomer). This disparity may arise from at least two differences between the experiments. First, the molecules studied in refs 4 and 6 are terminated with thiol groups, rather than pyridine groups. Thiols are known to form bonds to Au with strong coupling in a variety of motifs, while pyridines preferentially bind to undercoordinated atop sites.[21,28,29] Earlier work has reported conductance steps for 1,4-benzenedithiol junctions spanning the range from $10^{-5}\ G_0$ to as high as $10^{-1}\ G_0$ and no well-defined peak in the conductance histogram.[18] In contrast, benzene-based molecules with amine and pyridine end-groups yield histograms with relatively narrow peaks (with a peak width less than 1 order of magnitude) at lower conductances: 1,4-diaminobenzene shows a peak at $6.4 \times 10^{-3}\ G_0$[18,30] and 1,4-bis(4-pyridyl)benzene shows two peaks in the $10^{-5}\ G_0$ range.[22] Second, our results represent the full range of geometric configurations, while the authors of ref 6 constructed histograms with a subset of traces that showed distinct plateaus, so it is possible that their measured conductance values represent the "high" range of conductance for the thiol-terminated dithienylethene molecules.

To better understand the evolution and the range of conductance of our dithienylethene junctions, we constructed 2-dimensional histograms (binned in both conductance and in displacement) from our conductance data.[31] The displacement is measured from the point where the metallic Au junction first breaks so that the conductance drops below 1 G_0, and the data are binned at 0.02 nm intervals. The three panels of Figure 3 show data for bare Au in pure 1,2,4-trichlorobenzene solvent, and for compounds **1c** and **1o**, constructed from approximately 2000 traces each. All are plotted on the same color scale shown in Figure 3 panel a. The

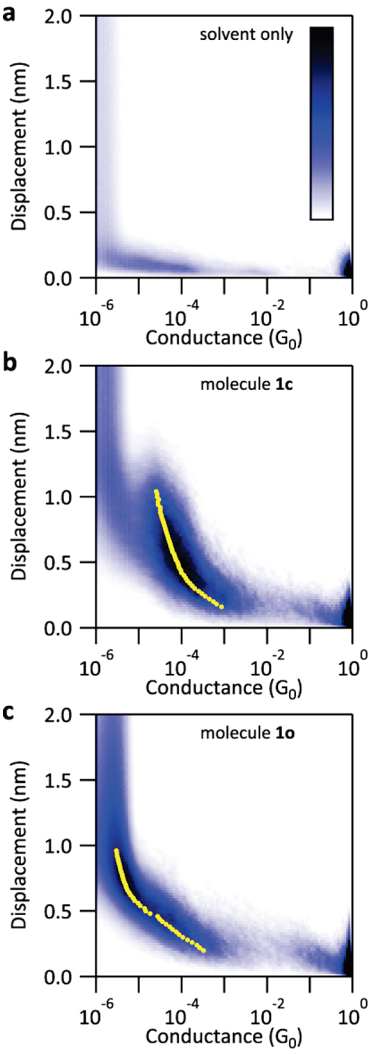

Figure 3. Comparison of logarithmically binned (in conductance) 2-dimensional histograms for (a) bare Au junctions in pure solvent, (b) 1o, and (c) 1c. The color scale (for counts) is linear and the same for all three plots. Counts are normalized to the number of traces. Yellow markers in panels b and c mark the peak position of the conductance histogram for each value of displacement (0.02 nm interval).

conductance is binned logarithmically.[21,31] We note that binning logarithmically without normalization to bin width[32] is equivalent to multiplying the regular-bin histogram by the conductance (with a multiplicative constant) which distorts and shifts the peak toward a higher conductance. Nevertheless, comparisons with histograms from bare Au electrodes (Figure 3a) confirm that the peak feature in Figure 3b is indeed associated with the molecule. Yellow dots in Figure 3b,c mark the conductance with the highest count for each displacement value and show a clear trend of decreasing conductance as the electrodes are pulled apart. This suggests that a range of conductance values are sampled as the molecule evolves in the junction from an askew geometry to a fully stretched geometry. For comparison, we have included the two-dimensional histogram for 4,4′-bipyridine in the

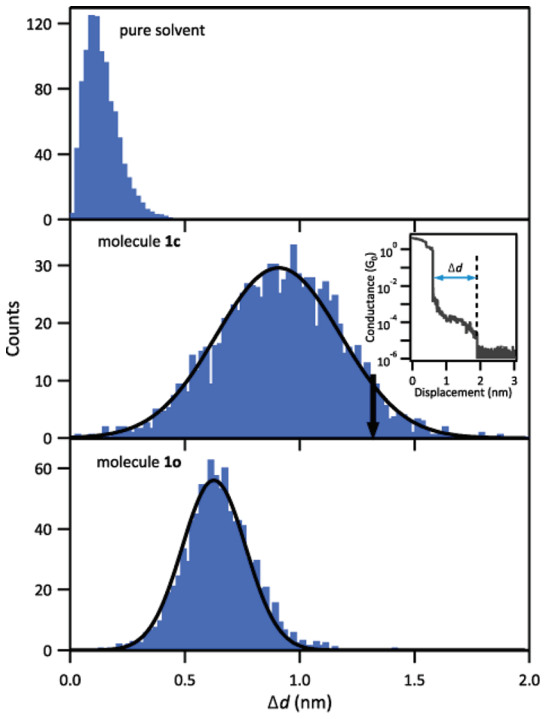

Figure 4. Histograms showing the distributions of the total displacement distance Δd (see inset for illustration) from the breaking of metallic atomic contact ($G < 1\ G_0$) to the noise level of the conductance measurement. Counts are normalized to 1000. Black solid lines are fits to Gaussian functions. The black arrow in the center panel indicates the 95th percentile of this displacement distribution.

Supporting Information, which also shows this same trend in conductance as a function of junction displacement.

Comparing the two-dimensional histograms of **1c** and **1o** (Figure 3b,c, respectively), we see two key differences: (1) **1c** has a higher conductance than **1o** across the relevant range of displacement and (2) the conductance feature for **1c** is separated from the noise (vertical feature at the left of the graph) whereas that of **1o** merges continuously with the noise band. As seen in the individual traces for **1o** (Figure S5 in Supporting Information), there is measurable current immediately following the breaking of the Au metallic contact, but the conductance is significantly lower than that for **1c**, and the fully stretched **1o** junction conductance appears to be below the noise level of our measurements.

A complementary way of viewing of these results is shown in Figure 4, which shows histograms for a quantity we will call the total displacement distance, Δd, equal to the distance between the breaking point of the metallic junction ($G < 1\ G_0$) and the point where the conductance drops below our instrumental noise level ($G < 3 \times 10^{-6}\ G_0$) (see inset). Data are shown for Au electrodes in pure solvent (top panel), and with **1c** (middle) and **1o** (bottom). The distributions of Δd are much broader for junctions with molecules, with peaks at greater values of displacement compared to the bare Au junctions. This confirms the presence of open molecules (**1o**) in the junctions despite the lack of a distinguishable feature in the conductance histogram for **1o** in Figure 2a.

As a reasonable estimate for the value of Δd for which the conductance of almost all of the **1c** junctions has fallen below noise level, we suggest taking the value of Δd at the 95th percentile, 1.32 nm (marked by a black arrow in Figure 4b). (Counts that fall beyond this value in the tail of the histogram may correspond to junctions in which the Au electrodes lengthen atypically due to thermal motion or strain.) The distance between Au electrodes immediately after the breaking of the metallic junction (the "snap-back" distance) is known to be 0.65 ± 0.25 nm.[33] The sum of this snap-back distance and the 95th percentile Δd for **1c** is therefore 2.0 ± 0.3 nm, which is, within experimental uncertainty, equal to the calculated length of this molecule, 1.99 nm (calculations are discussed below and in the Methods). This is consistent with a picture where the conductance peak we measure for **1c** corresponds to the molecule in the fully stretched configuration. The same analysis does not apply in the case of **1o**, for which the sum is 1.5 ± 0.3 nm, significantly different from the calculated length of 2.03 nm. For **1o** junctions, we were unable to measure current above the noise level beyond about 1.5 nm of electrode separation, so this comparison provides confirmation that the conductance for the fully stretched configuration of this molecule is below the measurement limit allowed by our noise floor.

The Venkataraman group has shown previously that some simple pyridine-terminated molecules exhibit bistable conductance.[22] The low-conductance state is associated with the molecule being fully stretched between the Au electrodes. The high-conductance state is a few times more conductive and is associated with the molecule being held at an angle within the junction, thereby providing greater orbital overlap with the neighboring Au atoms. We repeated the Venkataraman-group measurements[22] for 4,4′-bipyridine (BPY) and 1,2-bis(4-pyridyl)ethane (BPE) and confirmed the existence of bistable conductances for both (see Figure S3 in Supporting Information). However, in our measurements of the pyridine-terminated dithienylethene derivatives, we observe only one broad peak with no sign of bistability.

Since there is no reason to expect the bonding to Au of the pyridine group of the molecule **1c** to be different from that of BPY and BPE, the observation of only a single peak for **1c** suggests that the range of the high- and low-conductance peaks overlap significantly such that they are not individually resolvable. We investigated this hypothesis further by carrying out a set of DFT calculations for **1o** and **1c**. The conductances of a set of 182 optimized molecular junction configurations corresponding to different electrode separations (Figure 5a) were obtained within a nonequilibrium

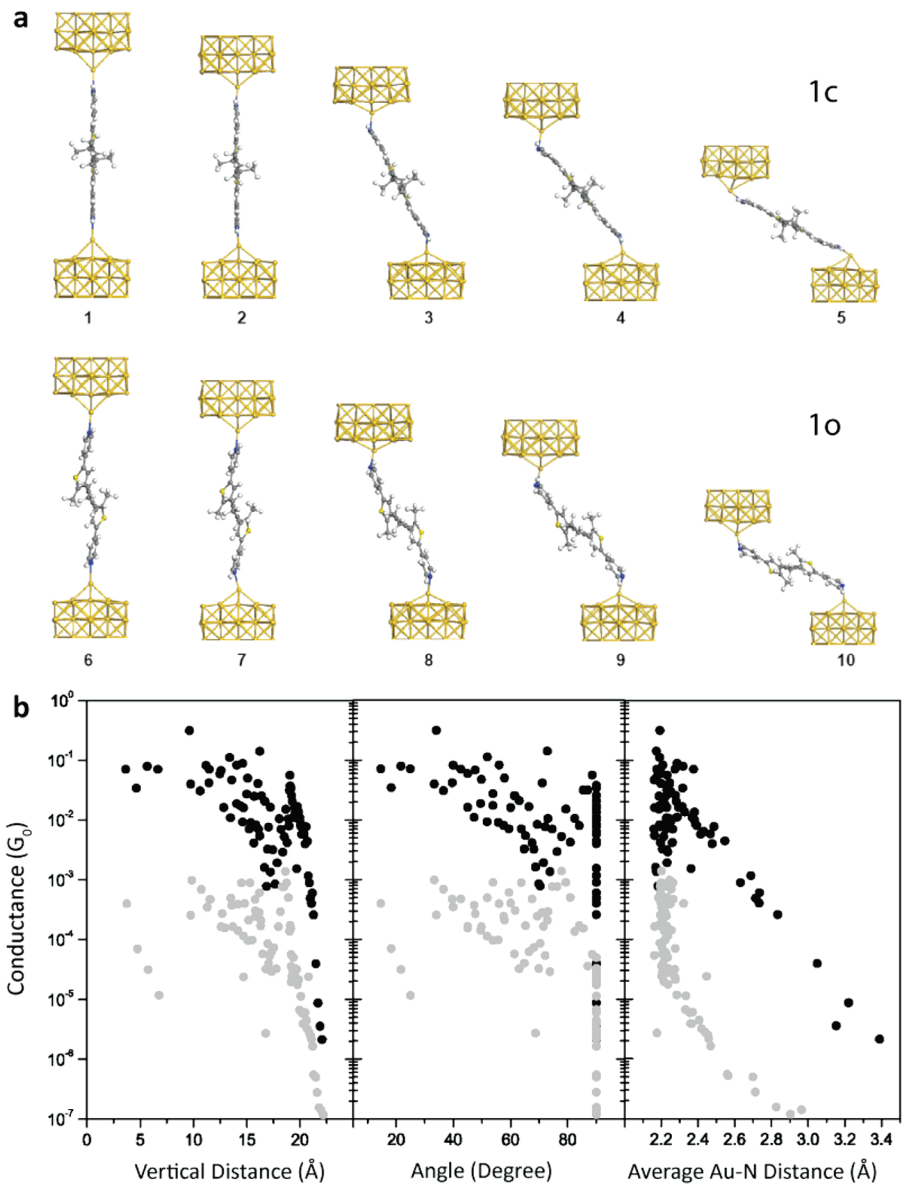

Figure 5. Conductance as a function of junction geometry obtained by density functional calculations on 182 relaxed molecular junctions. (a) Examples of molecular junctions with different electrode separations. Junctions 1−5 are examples for 1c, and 6−10 are examples for 1o. (b) Conductance of 1c (black circles) and 1o (gray circles) plotted against the electrode vertical distance, angle of the molecular junction, and N−Au distance.

Green's function DFT approach[34] (see Methods). Figure 5b shows a scatter-plot of the conductances as a function of electrode separation, angle between the molecule and the electrode, and N−Au distance. Although the calculated conductance values are much larger than found in experiment (due to well-known deficiencies in practical approximations to the functionals used to model conductance[35−39]), across a reasonable range of electrode separations we find that the conductance for **1c** is about 2 orders of magnitude larger than that of **1o**. This is consistent with our experimental limit for the on/off ratio. For the junction configurations considered, the calculated conductances vary smoothly with separation without any clear signs of bistability, again in agreement with our experimental findings.

CONCLUSION

We have applied the repeatedly formed break-junction technique to dithienylethene switch molecules terminated with pyridine linkers (molecules **1o**/**1c** and **2o**/**2c**) to achieve a better-defined molecular conductance than is possible with thiol linkers. Our statistical analyses employ histograms as a function of both conductance and electrode separation that represent the entire range of data, without any data selection. We find that the fully stretched Au−molecule−Au junction has a conductance in the 10^{-5} G_0 range for the closed form (**1c**) of the dithienylethene derivative, whereas the conductance for the open form (**1o**) is below our measurement limit of 10^{-6} G_0, giving an on/off ratio of at least 30, consistent with the results of our DFT

calculations. Unlike 4,4′-bipyridine and 1,2-bis(4-pyridyl)ethane, for which we find bistable conductance values consistent with published results, we observe only a single broad conductance peak for the dithienylethene derivative. Our findings are important for the application of this class of photochromic molecules in nanoscale electronic devices.

METHODS

Synthesis. Compounds **1o** and **2o** (Figure 1a) were prepared according to the procedures in refs 23−25 (see Figure S1 in the Supporting Information for a scheme of the synthesis protocol). All reactions were carried out under an atmosphere of dry nitrogen using standard Schlenk techniques. Dry tetrahydrofuran was distilled from sodium/benzophenone, and other solvents (analytical grade) were used without further purification. NMR solution spectra were recorded on a Varian 300 or Varian 400 spectrometer.

*Compound **1o**.* To a solution of 1,2-bis(5-chloro-2-methyl-3-thienyl)cyclopentene (compound **3** in Figure S1 in Supporting Information, 329 mg, 1.0 mmol) in THF (15 mL) was added 1.3 mL of 1.6 M *n*-butyllithium (2.0 mmol) in *n*-hexane at room temperature; 15 min later, 0.81 mL of tributyl borate (3.0 mmol) was added. After stirring for 1 h, the resulting reddish solution was used directly for the following addition. To another Schlenk flask filled with 25 mL of degassed DMSO was added 4-bromopyridine hydrochloride (436 mg, 2.2 mmol) and $Pd(PPh_3)_4$ (22 mg, 0.02 mmol). After the mixture was stirred for 15 min, 5 mL of 2 M aqueous sodium carbonate solution (10 mmol) and 0.5 mL of ethylene glycol were added. The solution was stirred for another 15 min under bubbling, before the temperature was raised to 60 °C. To the mixture was then added the above prepared reddish solution in one portion. The mixture was stirred at 80 °C for 24 h. After the mixture was cooled, 100 mL of toluene was added to dilute the mixture, followed by washing with water (20 mL × 2) and brine. Flash column chromatography on silica gel (ethyl acetate/hexane, 4/1) of the concentrated residue afforded 344 mg of **1o** as a solid in a yield of 83%. ^{1}H NMR data (300 MHz, $CDCl_3$) verifying the molecular identification: δ 2.01 (*s*, 6H, 2Me), 2.13 (*m*, 2H, $CH_2CH_2CH_2$), 2.85 (*t*, J = 7.5 Hz, 4H, $CH_2CH_2CH_2$), 7.21 (*s*, 2H, 2CH), 7.36 (*d*, J = 6.0 Hz, 4H), 8.52 (*d*, J = 5.7 Hz, 4H).

*Compound **2o**.* To a solution of 1,2-bis(5-chloro-2-methyl-3-thienyl)cyclopentene (compound **3** in Figure S1 in Supporting Information, 197 mg, 0.6 mmol) in THF (10 mL) was added 0.81 mL of 1.6 M *n*-butyllithium (1.3 mmol) in *n*-hexane at room temperature; 15 min later, 0.49 mL of tributyl borate (1.8 mmol) was added. After stirring for 1 h, the resulting reddish solution was used directly for the following addition. To another Schlenk flask filled with 20 mL of degassed DMSO was added 4-(4-bromophenyl)pyridine (304 mg, 1.3 mmol) and $Pd(PPh_3)_4$ (22 mg, 0.02 mmol). After stirring for 15 min, 3 mL of 2 M aqueous sodium carbonate solution (6 mmol) and 0.5 mL of ethylene glycol were added. The solution was stirred for another 15 min under bubbling, before the temperature was raised to 60 °C. To the mixture was then added the above prepared reddish solution in one portion. The mixture was stirred at 80 °C for 24 h. After the mixture was cooled, 100 mL of toluene was added to dilute the mixture, followed by washing with water (20 mL × 2) and brine. Flash column chromatography on silica gel (ethyl acetate/hexane, 4/1) of the concentrated residue afforded 100 mg of **2o** as a solid in a yield of 30%. Data verifying the molecular identification were ^{1}H NMR (300 MHz, $CDCl_3$): δ 2.04 (*s*, 6H, 2Me), 2.15 (*m*, 2H, $CH_2CH_2CH_2$), 2.87 (*t*, J = 7.2 Hz, 4H, $CH_2CH_2CH_2$), 7.13 (*s*, 2H, 2CH), 7.50 (*d*, J = 6.0 Hz, 4H), 7.62 (*s*, 8H). 8.65 (*d*, J = 5.7 Hz, 4H); ^{13}C NMR (75 MHz, $CDCl_3$): δ 14.79, 23.27, 38.71, 121.52, 124.91, 126.07, 127.65, 134.98, 135.62, 135.68, 136.44, 137.16, 138.89, 148.17, 148.59, 150.18.

Conductance Measurements. As prepared, the molecules are in the open form (**1o** and **2o**). A <1 mM solution is made with 1,2,4-trichlorobenzene, a high boiling point (214.4 °C) solvent. A solution of the closed-form molecules is prepared by irradiating the open-form solution with a light-emitting diode centered at 362 nm (~1500 μW/cm^2) for approximately 15 min. The conversion of the molecules to the closed form was verified by UV−vis spectroscopy, as shown in Figure 1.

For measuring the electrical conductance of the molecules, we use a tip freshly cut from 0.25 mm-diameter Au (99.999%) wire from Alfa Aesar. The wire is cleaned in acetone, rinsed in isopropyl alcohol and cleaned in an O_2 plasma before cutting. The substrate is an oxidized Si chip with 100 nm of Au (99.999%) deposited by electron-beam evaporation. The tip is biased at 25−100 mV and the current through the substrate is amplified with a DL 1211 current preamplifier with appropriate gain settings (1 μA/V to 1 nA/V). The output of the current preamplifier is read by a National Instruments PXI-4461 card at 40 kHz. A series resistor is sometimes added in the circuit and taken into account in the data processing. The tip is moved by a piezoelectric actuator with data recorded as the tip is withdrawn from the substrate. Every conductance *versus* displacement trace in which the junction breaks completely (implemented as requiring $G < 5 \times 10^{-6}\ G_0$) is binned into conductance histograms with evenly spaced bins (*i.e.*, a linear scale). The measurement cycle is automated to allow us to measure thousands of traces for each histogram.

To construct two-dimensional histograms as a function of both conductance and junction displacement,[21] we first take each conductance trace and define as zero displacement the data point at which the conductance drops and remains below 1 G_0. Each trace is then binned using a logarithmically spaced conductance scale and a linearly spaced displacement scale. Normalizing the counts to the respective conductance bin widths recovers the histogram obtained with linearly spaced bins. Comparison to control histograms (bare Au electrodes) shows that the peak is not an artifact of binning. The peak conductance at each displacement value (plotted as yellow markers in Figure 3b and as black circles in Figure S4 in the Supporting Information) was determined by taking a line cut at each displacement value and fitting to the peak.

Computations. We employed standard Kohn−Sham density functional theory (DFT) for the electronic structure using the Perdew−Burke−Ernzerhof (PBE) generalized gradient approximation exchange-correlation functional[40] and a local atomic orbital basis as implemented in the SIESTA code.[41,42] We used a double-ζ with polarization atomic basis throughout and norm-conserving pseudopotentials[43,44] in their fully nonlocal form.[45] The geometries of the molecular junctions were generated as follows. First we optimized isolated molecular structures of **1c** and **1o** with a single Au atom attached at a variety of N−Au bond distances and angles. The optimized fragments were then attached to Au[100] electrodes (with alternately 12 and 13 Au atoms per surface layer, configuration shown in Figure S6 in Supporting Information), and the molecule and the top two layers of the electrode were allowed to relax. These optimizations produced the large number of geometries used in the subsequent conductance calculations. Representative geometries are shown in Figure 5a.

In the fully relaxed geometry the N−Au distance was 0.224 nm for **1c** and 0.222 nm **1o**. Upon bringing the top and bottom Au electrodes together, the N−Au distance remains relatively unchanged and the compression is accommodated by increasing the angle between the molecular plane and the electrode (see Figure 5a); however, on pulling the electrodes apart, the N−Au distance increases to about 0.25 nm before the N−Au bond is broken. Computationally, the breaking of the junction was identified from the crossover of the single point energies of the molecule in the junction with the sum of the isolated junction and molecular energies.

To calculate the conductance, additional layers of Au atoms (at the experimental lattice parameter) were added (Figure S6 in the Supporting Information). The conductance calculations were carried out in the nonequilibrium Green's function DFT formalism, using a custom implementation on top of the SIESTA package. The implementation and formalism is described in detail in Ke *et al.*[46] The local density of states in a small window around the Fermi level (Figure S7, in the Supporting Information) shows that conductance proceeds primarily through the π-network of the molecule, in agreement with previous studies of related molecules.[11,14]

Acknowledgment. We thank L. Venkataraman, M. Kamenetska, J. Widawsky, D. Stewart, J. Tan, and S. Conte for technical help and discussions. We acknowledge funding from the NSF *via* the Cornell Center for Materials Research (NSF/DMR-0520404) and the Cornell Center for Chemical Interfacing, a Phase I Center for Chemical Innovation (NSF/CHE-0847926). E.S. T. was partially supported by the National Science and Engineering Research Council of Canada. M.B.S. acknowledges financial support from the Provost's Academic Diversity Postdoctoral Fellowship from Cornell University.

Supporting Information Available: Synthetic scheme, supporting data for the characterization of our apparatus, additional sample conductance traces for the dithienylethenes, computational figures, and brief discussion about the results of the calculations. This material is available free of charge *via* the Internet at http://pubs.acs.org.

REFERENCES AND NOTES

1. Irie, M. Diarylethenes for Memories and Switches. *Chem. Rev.* **2000**, *100*, 1685–1716.
2. Staykov, A.; Areephong, J.; R. Browne, W.; L. Feringa, B.; Yoshizawa, K. Electrochemical and Photochemical Cyclization and Cycloreversion of Diarylethenes and Diarylethene-Capped Sexithiophene Wires. *ACS Nano* **2011**, *5*, 1165–1178.
3. Jan van der Molen, S.; Liljeroth, P. Charge Transport through Molecular Switches. *J. Phys.: Condens. Matter* **2010**, *22*, 133001.
4. Dulić, D.; van der Molen, S. J.; Kudernac, T.; Jonkman, H. T.; de Jong, J. J. D.; Bowden, T. N.; van Esch, J.; Feringa, B. L.; van Wees, B. J. One-Way Optoelectronic Switching of Photochromic Molecules on Gold. *Phys. Rev. Lett.* **2003**, *91*, 207402.
5. van der Molen, S. J.; Liao, J.; Kudernac, T.; Agustsson, J. S.; Bernard, L.; Calame, M.; van Wees, B. J.; Feringa, B. L.; Schönenberger, C. Light-Controlled Conductance Switching of Ordered Metal−Molecule−Metal Devices. *Nano Lett.* **2009**, *9*, 76–80.
6. He, J.; Chen, F.; Liddell, P. A.; Andréasson, J.; Straight, S. D.; Gust, D.; Moore, T. A.; Moore, A. L.; Li, J.; Sankey, O. F.; Lindsay, S. M. Switching of a Photochromic Molecule on Gold Electrodes: Single-Molecule Measurements. *Nanotechnology* **2005**, *16*, 695–702.
7. Katsonis, N.; Kudernac, T.; Walko, M.; van der Molen, S. J.; van Wees, B. J.; Feringa, B. L. Reversible Conductance Switching of Single Diarylethenes on a Gold Surface. *Adv. Mater.* **2006**, *18*, 1397–1400.
8. Whalley, A. C.; Steigerwald, M. L.; Guo, X.; Nuckolls, C. Reversible Switching in Molecular Electronic Devices. *J. Am. Chem. Soc.* **2007**, *129*, 12590–12591.
9. Matsuda, K.; Yamaguchi, H.; Sakano, T.; Ikeda, M.; Tanifuji, N.; Irie, M. Conductance Photoswitching of Diarylethene−Gold Nanoparticle Network Induced by Photochromic Reaction. *J. Phys. Chem. C* **2008**, *112*, 17005–17010.
10. Kudernac, T.; Molen, S. J. van der; Wees, B. J. van; Feringa, B. L. Uni- and Bi-directional Light-Induced Switching of Diarylethenes on Gold Nanoparticles. *Chem. Commun.* **2006**, 3597–3599.
11. Li, J.; Speyer, G.; Sankey, O. F. Conduction Switching of Photochromic Molecules. *Phys. Rev. Lett.* **2004**, *93*, 248302.
12. Kondo, M.; Tada, T.; Yoshizawa, K. A Theoretical Measurement of the Quantum Transport through an Optical Molecular Switch. *Chem. Phys. Lett.* **2005**, *412*, 55–59.
13. Odell, A.; Delin, A.; Johansson, B.; Rungger, I.; Sanvito, S. Investigation of the Conducting Properties of a Photoswitching Dithienylethene Molecule. *ACS Nano* **2010**, *4*, 2635–2642.
14. Zhuang, M.; Ernzerhof, M. Mechanism of a Molecular Electronic Photoswitch. *Phys. Rev. B* **2005**, *72*, 073104.
15. Evers, F.; Weigend, F.; Koentopp, M. Conductance of Molecular Wires and Transport Calculations Based on Density-Functional Theory. *Phys. Rev. B* **2004**, *69*, 235411.
16. Tian, H.; Yang, S. Recent Progresses on Diarylethene Based Photochromic Switches. *Chem. Soc. Rev.* **2004**, *33*, 85–97.
17. Nichols, R. J.; Haiss, W.; Higgins, S. J.; Leary, E.; Martin, S.; Bethell, D. The Experimental Determination of the Conductance of Single Molecules. *Phys. Chem. Chem. Phys.* **2010**, *12*, 2801.
18. Venkataraman, L.; Klare, J. E.; Tam, I. W.; Nuckolls, C.; Hybertsen, M. S.; Steigerwald, M. L. Single-Molecule Circuits with Well-Defined Molecular Conductance. *Nano Lett.* **2006**, *6*, 458–462.
19. Xu, B.; Tao, N. J. Measurement of Single-Molecule Resistance by Repeated Formation of Molecular Junctions. *Science* **2003**, *301*, 1221–1223.
20. Venkataraman, L.; Klare, J. E.; Nuckolls, C.; Hybertsen, M. S.; Steigerwald, M. L. Dependence of Single-Molecule Junction Conductance on Molecular Conformation. *Nature* **2006**, *442*, 904–907.
21. Quek, S. Y.; Kamenetska, M.; Steigerwald, M. L.; Choi, H. J.; Louie, S. G.; Hybertsen, M. S.; Neaton, J. B.; Venkataraman, L. Mechanically Controlled Binary Conductance Switching of a Single-Molecule Junction. *Nat. Nano.* **2009**, *4*, 230–234.
22. Kamenetska, M.; Quek, S. Y.; Whalley, A. C.; Steigerwald, M. L.; Choi, H. J.; Louie, S. G.; Nuckolls, C.; Hybertsen, M. S.; Neaton, J. B.; Venkataraman, L. Conductance and Geometry of Pyridine-Linked Single-Molecule Junctions. *J. Am. Chem. Soc.* **2010**, *132*, 6817–6821.
23. Qin, B.; Yao, R.; Zhao, X.; Tian, H. Enhanced Photochromism of 1,2-Dithienylcyclopentene Complexes with Metal Ion. *Org. Biomol. Chem.* **2003**, *1*, 2187.
24. Lucas, L. N.; Jong, J. J. D. de; Esch, J. H. van; Kellogg, R. M.; Feringa, B. L. Syntheses of Dithienylcyclopentene Optical Molecular Switches. *Eur. J. Org. Chem.* **2003**, *2003*, 155–166.
25. Zhong, Y.-W.; Vila, N.; Henderson, J. C.; Abruña, H. D. Dithienylcyclopentenes-Containing Transition Metal Bisterpyridine Complexes Directed toward Molecular Electronic Applications. *Inorg. Chem.* **2009**, *48*, 991–999.
26. Hybertsen, M. S.; Venkataraman, L.; Klare, J. E.; Whalley, A. C.; Steigerwald, M. L.; Nuckolls, C. Amine-Linked Single-Molecule Circuits: Systematic Trends across Molecular Families. *J. Phys.: Condens. Matter* **2008**, *20*, 374115.
27. Wang, C.; Batsanov, A. S.; Bryce, M. R.; Martín, S.; Nichols, R. J.; Higgins, S. J.; García-Suárez, V. M.; Lambert, C. J. Oligoyne Single Molecule Wires. *J. Am. Chem. Soc.* **2009**, *131*, 15647–15654.
28. Basch, H.; Cohen, R.; Ratner, M. A. Interface Geometry and Molecular Junction Conductance: Geometric Fluctuation and Stochastic Switching. *Nano Lett.* **2005**, *5*, 1668–1675.
29. Strange, M.; Lopez-Acevedo, O.; Häkkinen, H. Oligomeric Gold−Thiolate Units Define the Properties of the Molecular Junction between Gold and Benzene Dithiols. *J. Phys. Chem. Lett.* **2010**, *1*, 1528–1532.
30. Ulrich, J.; Esrail, D.; Pontius, W.; Venkataraman, L.; Millar, D.; Doerrer, L. H. Variability of Conductance in Molecular Junctions. *J. Phys. Chem. B* **2006**, *110*, 2462–2466.
31. Kamenetska, M.; Koentopp, M.; Whalley, A. C.; Park, Y. S.; Steigerwald, M. L.; Nuckolls, C.; Hybertsen, M. S.; Venkataraman, L. Formation and Evolution of Single-Molecule Junctions. *Phys. Rev. Lett.* **2009**, *102*, 126803.
32. González, M. T.; Wu, S.; Huber, R.; van der Molen, S. J.; Schönenberger, C.; Calame, M. Electrical Conductance of Molecular Junctions by a Robust Statistical Analysis. *Nano Lett.* **2006**, *6*, 2238–2242.
33. Yanson, A. I.; Bollinger, G. R.; van den Brom, H. E.; Agrait, N.; van Ruitenbeek, J. M. Formation and Manipulation of a

Metallic Wire of Single Gold Atoms. *Nature* **1998**, *395*, 783–785.
34. Zhou, X.-S.; Chen, Z.-B.; Liu, S.-H.; Jin, S.; Liu, L.; Zhang, H.-M.; Xie, Z.-X.; Jiang, Y.-B.; Mao, B.-W. Single Molecule Conductance of Dipyridines with Conjugated Ethene and Nonconjugated Ethane Bridging Group. *J. Phys. Chem. C* **2008**, *112*, 3935–3940.
35. Di Ventra, M.; Pantelides, S. T.; Lang, N. D. First-Principles Calculation of Transport Properties of a Molecular Device. *Phys. Rev. Lett.* **2000**, *84*, 979.
36. Delaney, P.; Greer, J. C. Correlated Electron Transport in Molecular Electronics. *Phys. Rev. Lett.* **2004**, *93*, 036805.
37. Ke, S.-H.; Baranger, H. U.; Yang, W. Role of the Exchange-Correlation Potential in *ab Initio* Electron Transport Calculations. *J. Chem. Phys.* **2007**, *126*, 201102.
38. Sai, N.; Zwolak, M.; Vignale, G.; Di Ventra, M. Dynamical Corrections to the DFT-LDA Electron Conductance in Nanoscale Systems. *Phys. Rev. Lett.* **2005**, *94*, 186810.
39. Toher, C.; Filippetti, A.; Sanvito, S.; Burke, K. Self-Interaction Errors in Density-Functional Calculations of Electronic Transport. *Phys. Rev. Lett.* **2005**, *95*, 146402.
40. Perdew, J. P.; Burke, K.; Ernzerhof, M. Generalized Gradient Approximation Made Simple. *Phys. Rev. Lett.* **1996**, *77*, 3865.
41. Sánchez-Portal, D.; Ordejón, P.; Artacho, E.; Soler, J. M. Density-Functional Method for Very Large Systems with LCAO Basis Sets. *Int. J. Quantum Chem.* **1997**, *65*, 453–461.
42. Soler, J. M.; Artacho, E.; Gale, J. D.; García, A.; Junquera, J.; Ordejón, P.; Sánchez-Portal, D. The SIESTA Method for *ab Initio* Order-*N* Materials Simulation. *J. Phys.: Condens. Matter* **2002**, *14*, 2745.
43. Hamann, D. R.; Schlüter, M.; Chiang, C. Norm-Conserving Pseudopotentials. *Phys. Rev. Lett.* **1979**, *43*, 1494.
44. Bachelet, G. B.; Hamann, D. R.; Schlüter, M. Pseudopotentials that work: From H to Pu. *Phys. Rev. B* **1982**, *26*, 4199.
45. Kleinman, L.; Bylander, D. M. Efficacious Form for Model Pseudopotentials. *Phys. Rev. Lett.* **1982**, *48*, 1425.
46. Ke, S.-H.; Baranger, H. U.; Yang, W. Electron Transport through Molecules: Self-Consistent and Non-Self-Consistent Approaches. *Phys. Rev. B* **2004**, *70*, 085410.